

Catalytic activity of rhodium complexes supported on $\text{Al}_2\text{O}_3\text{--ZrO}_2$ in isomerization and hydroformylation of 1-hexene

Józef Wrzyszcza^{a,*}, Mirosław Zawadzki^a, Anna M. Trzeciak^b, Włodzimierz Tylus^c, and Józef J. Ziolkowski^b

^a*Institute of Low Temperature and Structure Research Polish Academy of Sciences, P.O. Box 937, 50-950 Wrocław, Poland*

^b*Faculty of Chemistry, University of Wrocław, 14 F. Joliot-Curie, 50-383 Wrocław, Poland*

^c*Wrocław University of Technology, Institute of Inorganic Technology, Wybrzeże Wyspiańskiego 27, 50-370 Wrocław, Poland*

Received 23 September 2003; accepted 9 December 2003

Two new nanostructured $\text{Al}_2\text{O}_3\text{--ZrO}_2$ mixed oxides supports, A and B, have been prepared by sol–gel process and characterized by TEM, XRD and XPS methods. The freeze-dried gel gave support A whereas the support B was obtained by drying of gel at ambient temperature. Both supports reacted with $\text{Rh}(\text{acac})(\text{CO})_2$ complex, producing $\text{Rh}(\text{CO})_2^+$ tethered species, characterized by $\nu(\text{CO})$ at 2011 and 2083 cm^{-1} . The $\text{Rh}(\text{CO})_2^+/\text{A}$ applied as catalyst for reaction of 1-hexene at 80 °C with $\text{H}_2/\text{CO} = 1$, at 10 atm was found as active for isomerization (ca. 90% of 2-hexene after 6 h) and relatively poor catalyst of hydroformylation (< 10% of aldehydes). At the presence of stoichiometric amount of PPh_3 the yield of aldehydes increased up to 65%. The selectivity of the reaction was strongly dependent on the catalyst pre-treatment with CO or CO/H_2 mixture.

KEY WORDS: nanostructured $\text{Al}_2\text{O}_3\text{--ZrO}_2$ oxides; supported rhodium complexes; hydroformylation; XPS.

1. Introduction

Immobilization of homogeneous organometallic catalysts on various carriers, both, organic (i.e. polymers, ionic exchange resins) and inorganic (i.e. silica, metal oxides, zeolites) shows since many years of permanently growing interest [1]. Although, immobilization of active homogeneous organometallic catalysts usually leads to the catalytic systems of lower activity, nevertheless the problems of separation and stability of catalysts are obvious advantages of heterogenized systems [1–3]. It should be mentioned however, that leaching of the metal from support is an important disadvantage in application of immobilized catalysts in practice.

In recent years the active and selective catalysts have been prepared by immobilization of rhodium complexes on functionalized silicas [4–10]. We have prepared an active catalyst of hydroformylation by heterogenization of rhodium complex on spinel, ZnAl_2O_4 [11].

The limited possibility of Rh complexes heterogenization on alumina has been reported in our other work: only hydroxy-rhodium complexes could be effectively attached to the support surface [12]. Continuing studies on tethered rhodium complexes we have prepared alternative nanostructured support composed by alumina–zirconia solid solution which surface and catalytic properties could be different from those of pure alumina [13].

In this paper we report results of structural studies of the support and supported rhodium complexes as well as results of their application as catalysts of hydroformylation and isomerization of 1-hexene.

2. Experimental

2.1. Synthesis of alumina–zirconia support

To prepare the nanostructured $\text{Al}_2\text{O}_3\text{--ZrO}_2$ mixed oxides support, 102 g of aluminum iso-propoxide was hydrolyzed in excess of distilled water heated at 75 °C for 15 min. Such obtained aluminum hydroxide was peptized by slow addition of zirconium nitrate aqueous solution until the desired concentration was reached (10 wt% zirconia content). The preparation was then left under stirring and refluxing at 98 °C for 24 h. The obtained clear sol was left at room temperature until gel was formed which was then divided into two parts. One part (A) was freeze-dried while the other, (B), was dried at ambient temperature for several days giving transparent thin material. Both samples, (A) and (B), were heat-treated at 600 °C to obtain alumina–zirconium mixed oxides which were used as supports A and B for $[\text{Rh}(\text{acac})(\text{CO})_2]$ and $[\text{Rh}(\text{acac})(\text{CO})(\text{PPh}_3)]$ complexes.

2.2. Methods of support characterization

The structure and phase compositions of the support material were determined by using CuK_α radiation from a DRON 3 powder diffractometer. The average crystallite sizes in Al_2O_3 were determined using Scherrer formula from the half-widths of the alumina (400) X-ray reflections. The BET specific surface area and porosity were estimated by nitrogen adsorption at 77 K using an automatic volumetric apparatus Fisons Sorptomatic 1900. Samples were previously degassed for 4 h at 250 °C and 10^{-3} Tr. The pore size distribution was analyzed following the Dollimore–Heal method, assum-

* To whom correspondence should be addressed.

ing a cylindrical pore model. The particle sizes and morphology of the support material were estimated from TEM images taken with a TESLA BS-500 transmission electron microscope using an accelerating voltage of 90 kV. Scanning electron microscope Philips 515 equipped with EDAX analysis was used to examine the morphology of support material as well as to determine the surface concentration of the Rh ions.

XPS spectra were recorded on SPECS UHV/XPS/AES system using MgK_{α} source for excitation and equipped with a hemispherical analyzer operating in fixed analyzer transmission mode with pass energy 10 or 20 eV. A power setting of 10 kV and 120 W was applied. The working pressure in an analyzing chamber was less than $5 \cdot 10^{-10}$ mbar. The binding energy (BE) scale was calibrated by taking the Au $4f_{7/2}$ peak at 84 eV. Correction of the energy shift due to the static charging of the samples was accomplished using as reference the C1s peak at 284.8 eV. The accuracy of the reported BE was ± 0.1 eV. For the XPS analysis, all sample specimens were obtained by pressing sample powders into thin disks which were mounted on sample holders and placed in a prechamber, outgassed to less than 10^{-8} mbar at room temperature, and then transferred to the analysis chamber. Stability of Rh spectra during the XPS measurements was proved by a series of successive measurements. The spectra were collected and processed by SpecsLab software. The data analysis procedure involved data smoothing and background calculation using the Voight function which is a convolution of Gaussian instrumental function and Lorentzian function for the natural line shape.

2.3. Synthesis and heterogenization of rhodium complexes

Rhodium complexes have been prepared according to literature methods: $Rh(acac)(CO)_2$ [14], $Rh(acac)(CO)(PPh_3)$ [15].

Rhodium complexes: $[Rh(acac)(CO)_2]$ **1** and $[Rh(acac)(CO)(PPh_3)]$ **2**, were heterogenized on A and B supports by impregnation from the toluene solutions at room temperature. The impregnation process of **1** was monitored by UV-vis spectra measurements. After 24 h the impregnation process was completed and amounts of rhodium attached to the support was estimated from absorption change. Independently, rhodium content was determined by ICP method (after conversion of the grafted rhodium complex into solution with hydrochloric acid) and EDAX method (table 3). For the samples of **2** supported on Al_2O_3 - ZrO_2 support only ICP and EDAX methods have been used.

2.4. Hydroformylation and isomerization reactions

Hydroformylation and isomerization reactions have been performed in a steel autoclave (40 cm^3) with magnetic stirrer at $80\text{ }^\circ\text{C}$ and 10 atm $H_2/CO = 1$.

Supported catalysts before use were stabilized by refluxing in toluene for 2 h, filtration, washing with toluene and drying in vacuo. A suitable amount of catalyst in small Teflon vessel, 1.5 cm^3 of toluene and 1.5 cm^3 of 1-hexene were introduced to the autoclave in N_2 atmosphere. Autoclave was closed, filled first with H_2 (5 atm) and with CO up to 10 atm. After the reaction (4–6 h) the autoclave was cooled down and the liquid sample was analyzed by GC-MS on GC-MS Hewlett-Packard instrument: HP 5890 II chromatograph with mass detector HP 5971a.

3. Results and discussion

3.1. Characterization of alumina–zirconia support

The phase identification in the material prepared through sol-gel process was performed by means of X-ray diffraction techniques for as-prepared samples and after calcination the samples (A and B) for 3 h at $600\text{ }^\circ\text{C}$. The XRD results for sample B are identical to those shown on figure 1 for sample A. For fresh dried samples a typical pseudoboehmite ($AlOOH$) pattern was obtained, which is characteristic for material prepared by hot water hydrolysis of alkoxides. A broad diffraction peak with two maxima at $2\theta = 32^\circ$ and 37.5° is observed for samples calcined at $600\text{ }^\circ\text{C}$, together with two peaks at 46° and 67° , which are characteristic peaks corresponding to the (220)/(311), (400), and (440) reflections of γ - Al_2O_3 ; none zirconia phase was detected. Crystallization of tetragonal zirconia in such system occurs at temperatures above $600\text{ }^\circ\text{C}$ and two separate phases – corundum and zirconia – are well observed after heat treatment at $1200\text{ }^\circ\text{C}$. ZrO_2 seems therefore to form metastable solid solution with the alumina matrix after calcining at $600\text{ }^\circ\text{C}$. The average size of the γ - Al_2O_3 particles determined by XRD analysis was 7 nm.

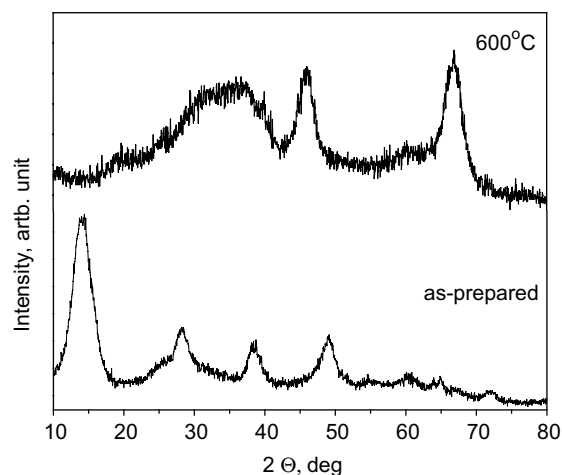


Figure 1. XRD pattern of alumina–zirconia support (sample A): as-prepared and heated at $600\text{ }^\circ\text{C}$ for 3 h.

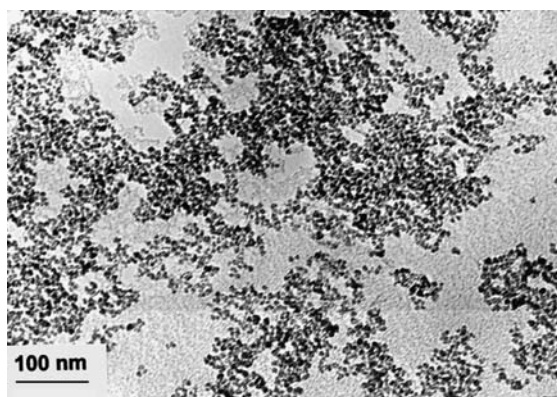


Figure 2. TEM image of as-prepared sample of alumina-zirconia sol.

The particle size and shape of as prepared and calcinated samples were investigated by TEM. The morphology of alumina-zirconia sol shown on figure 2 is quite homogenous and sol consists of uniform quasi-spherical particles of an average size of 5 nm. The sample A, obtained by freeze drying, consists of macroporous lumps shown in figure 3. The morphology of samples A and B (after heat treatment at 600 °C) are similar but particles are more or less aggregated and its average sizes are 6–7 nm, in good agreement with XRD patterns.

The main textural properties of alumina-zirconia supports A and B obtained from adsorption-desorption N_2 -isotherms are collected in table 1. The typical nitrogen adsorption-desorption isotherms and pore size



Figure 3. SEM picture of freeze-dried alumina-zirconia gel (sample A).

Table 1

Some textural properties (specific surface area S_{BET} , pore volume V_p , mean pore diameter D_p) of alumina-zirconia supports A and B (heat treated at 600 °C)

Support	S_{BET} (m ² /g)	V_p (cm ³ /g)	D_p (nm)
As-prepared	192	0.10	< 1
A	215	0.27	2.0
B	165	0.19	1.8

distribution for studied samples are shown in figure 4. The analysis of the obtained isotherms leads to identification of their profiles, as Type I for as-prepared sample and Type IV for samples heat treated at 600 °C (A and B). The first one is typical for the microporous materials while the second one, with closed hysteresis loops described as type H1 or H2, is typical for the mesoporous materials. These types of hysteresis loops are characteristic for solids consisting of particles crossed by nearly cylindrical channels or made by aggregates or agglomerates of nearly spheroidal particles. Moreover, such hysteresis loops suggest that pores can have uniform size and shape. The analysis of the pore size distribution profiles for the Al_2O_3 - ZrO_2 samples suggests that pore size distribution is monomodal for A and B samples, centered at 1.8 and 2.1 nm, respectively. Very narrow pore size range for both samples suggest that sol-gel prepared material is formed from monodispersed particles.

The BE determined for support A by XPS method for Zr 3d_{3/2} and Al 2p_{3/2} were equal 182.1 and 74 eV, respectively what confirmed the presence of ZrO_2 and Al_2O_3 oxides. Corresponding BE for support B are slightly shifted towards higher values and equal 182.2 and 74.1 eV, respectively. Surface atomic ratio Zr/Al was equal 0.077 for support A and 0.08 for support B (table 2). These values are approximating to the volume ratio, equal 0.1 and observed small discrepancy may suggest small difference in the composition on the surface and in deep inside of the support.

Investigation of the sample of support A, first kept for few hours in toluene and next vacuum dried, shown significant amounts of toluene remained adsorbed, which BE C1s was equal 291.6 eV (figure 5). Contribution of “toluene” carbon in total amount of carbon in the sample warmed up in toluene at 80 °C for 2 h and next vacuum dried was 31.5% (figure 5a). When the sample was heated in CO atmosphere only 16% of “toluene” carbon was found adsorbed in the support A (figure 5b). The samples of support A containing rhodium complex are adsorbing significantly smaller amounts of toluene (figure 5c and d).

3.2. Characterization of rhodium complexes supported on alumina-zirconia support

The results of rhodium analyses collected in table 3 show very good agreement of the analytical methods used. It is also worth to note, that complex **1** is more efficiently impregnated than complex **2** – probably because of higher steric hindrance effect of bulky triphenylphosphine ligand.

Relatively low occupation of supports surface with rhodium made interpretation of XPS spectra difficult. To prevent Rh(I) to Rh(0) reduction low energy beam X-gun – 150 W (10 keV) was applied. BE values and surface atomic ratios are given in table 2. Deconvolu-

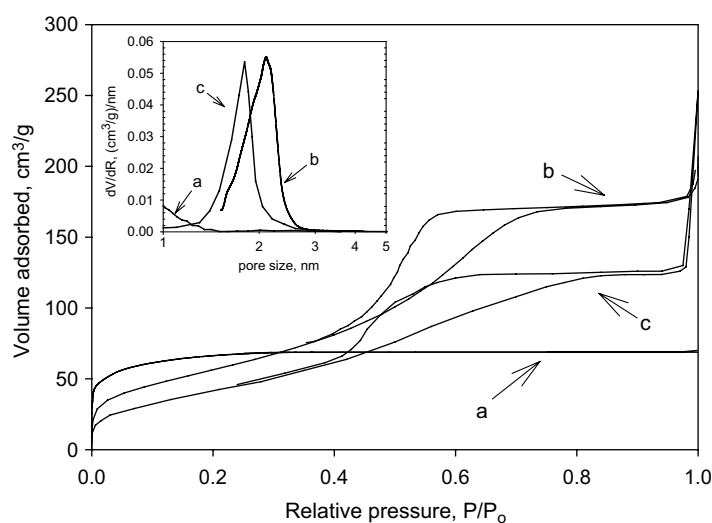


Figure 4. Adsorption-desorption isotherms of nitrogen at $-196\text{ }^{\circ}\text{C}$ and corresponding pore size distribution for alumina-zirconia support: (a) as-prepared; (b) heated at $600\text{ }^{\circ}\text{C}$ (sample A); (c) heated at $600\text{ }^{\circ}\text{C}$ (sample B).

Table 2
XPS surface atomic ratio and BE of Rh 3d core electrons (eV)

Catalyst	Zr/Al	Rh/Zr	P/Rh	Rh 3d _{5/2}
Rh(CO) ₂ ⁺ /B	0.083	0.096		309.61
Rh(CO) ₂ ⁺ /A	0.075	0.15		309.45
Rh(CO)P ⁺ /B	0.077	0.056		309.75
Rh(CO)P ⁺ /A	0.082	0.035	0.6	309.55
Rh(CO) ₂ ⁺ /A + H ₂ /CO + toluene ^a	0.085	0.14		309.0
Rh(CO) ₂ ⁺ /A + PPh ₃ + H ₂ /CO + 1-hexene + toluene ^a	0.087	0.17		309.23
Support A	0.077			
Support B	0.08			

^a Sample was heated at $80\text{ }^{\circ}\text{C}$ under 10 atm of H₂/CO for 2 h.

Table 3
Content of rhodium (%) in the samples of Rh(acac)(CO)₂ and Rh(acac)(CO)(PPh₃) supported on A and B carriers

Catalyst	Method of analysis					
	Fresh sample	Sample refluxed in toluene (2.5 h)		Sample refluxed in toluene with PPh ₃ ^a (2.5 h)		
	UV-vis	ICP	EDAX	ICP	EDAX	
Rh(CO) ₂ ⁺ /A	1.25	1.26	1.24	1.05	1.19	0.94
Rh(CO) ₂ ⁺ /B	1.53	1.41	1.60	1.43	1.28	1.10
Rh(CO)P ⁺ /A	0.32	0.34	—	—	—	0.15
Rh(CO)P ⁺ /B	0.6	0.5	—	0.4	—	0.35

^a 20-fold excess.

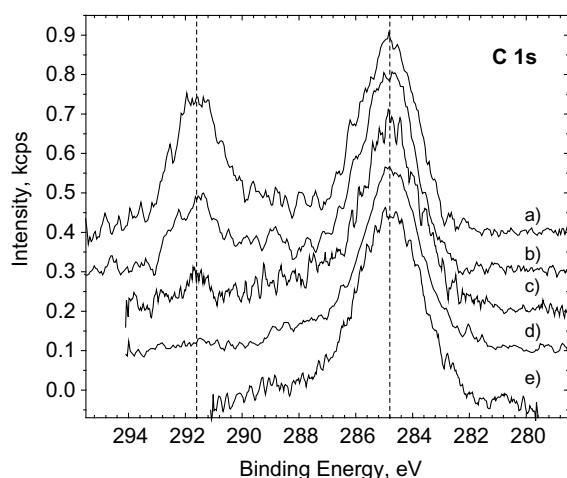


Figure 5. C 1s core-level spectra of selected samples: (a) A + toluene; (b) A + toluene + CO; (c) Rh(CO)₂⁺/A + H₂/CO ($80\text{ }^{\circ}\text{C}$, 10 atm, 2 h); (d) Rh(CO)₂⁺/A + PPh₃ + H₂/CO ($80\text{ }^{\circ}\text{C}$, 10 atm, 2 h); (e) Rh(CO)₂⁺/A.

tion of peaks revealed small differences in BE Rh 3d_{3/2} in the complex containing phosphine and phosphine-free one (309.45 eV for Rh(CO)₂⁺/A versus 309.58 eV for Rh(CO)P⁺/A ($\pm 0.1\text{ eV}$). Identical difference in BE was observed for complexes immobilized on support B (figure 6). Deconvolution was done at the assumption that both, the shape of curves (80% Lorentz), and FWHM in spin pairs are the same and d_{3/2}:d_{1/2} peak intensity ratio is constant and equal 3:2 (figure 6).

XPS spectrum of phosphorus was allowed to measure only for the sample Rh(CO)P⁺/A with theoretical P:Rh ratio equal 1:1. Experimentally determined ratio was lower and equal 0.6:1 (table 2). It maybe assumed that this value is underestimated due to quite complicated procedure of P 2p from Al 2s spectra separation. The P 2p spectrum in demand was obtained by the subtraction the support A spectrum from the spectrum of Rh(CO)P⁺/A (both spectra standardized) (figure 7).

In the IR spectra of supported complex **1** two $\nu(\text{CO})$ frequencies of similar intensity at $2011\text{ and }2083\text{ cm}^{-1}$

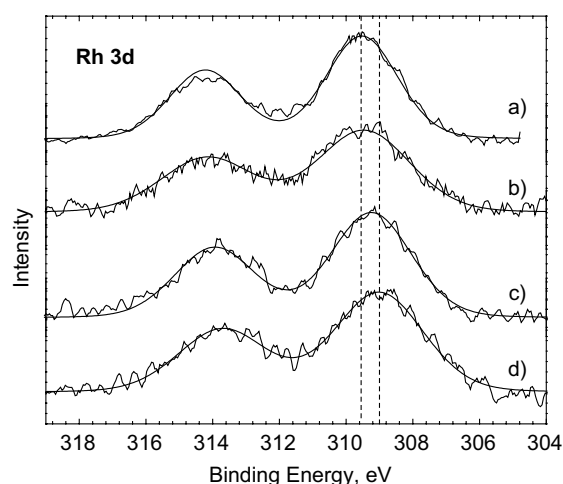


Figure 6. Rh 3d core-level spectra of selected samples: (a) $\text{Rh}(\text{CO})(\text{PPh}_3)^+/\text{A}$; (b) $\text{Rh}(\text{CO})_2^+/\text{A}$; (c) $\text{Rh}(\text{CO})_2^+/\text{A} + \text{PPh}_3 + \text{H}_2/\text{CO}$ (80 °C, 10 atm, 2 h); (d) $\text{Rh}(\text{CO})_2^+/\text{A} + \text{H}_2/\text{CO}$ (80 °C, 10 atm, 2 h).

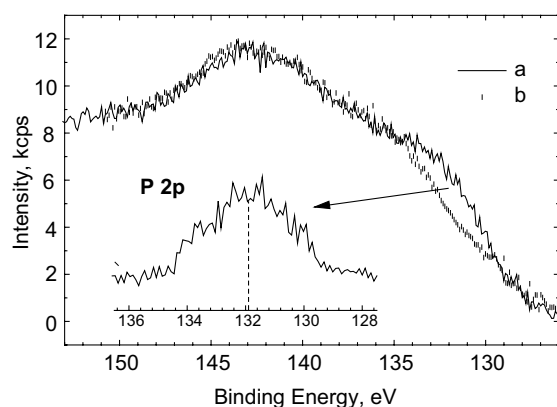
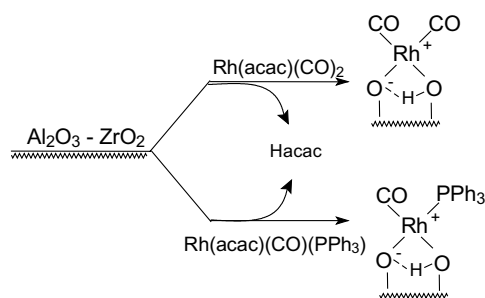


Figure 7. XPS narrow scans for $\text{Rh}(\text{CO})(\text{PPh}_3)^+/\text{A}$ (a) and support A (b); below P 2p core-level spectra extracted.

are observed, which are consistent with the presence of $\text{Rh}(\text{CO})_2^+$ species (scheme 1).

Almost identical $\text{Rh}(\text{CO})_2^+$ cationic species was observed on spinel ZnAl_2O_4 , ($\nu(\text{CO})$ 2015 and 2088 cm^{-1} respectively). Slightly higher values of $\nu(\text{CO})$ may suggest weaker donor properties of ZnAl_2O_4 spinel oxygens towards rhodium and in consequence



Scheme 1.

weaker rhodium back-bonding to CO. IR spectra of samples aged several days showed gradual decrease of $\nu(\text{CO})$ intensity up to the total disappearance. This effect, identical to the earlier observed for $\text{Rh}(\text{CO})_2^+$ supported on spinel ZnAl_2O_4 , is caused by CO oxidation to CO_2 . The catalyst can be regenerated and $\nu(\text{CO})$ frequencies are observed again when the sample is left in CO atmosphere.

The sample of catalyst obtained by the support impregnation with $[\text{Rh}(\text{acac})(\text{CO})(\text{PPh}_3)]$ shows in IR spectrum only one $\nu(\text{CO})$ frequency at 1980 cm^{-1} , characteristic for anchored $\text{Rh}(\text{CO})(\text{PPh}_3)^+$ species (scheme 1). The same species was also formed in reaction of supported $\text{Rh}(\text{CO})_2^+$ with PPh_3 . It is however interesting to note, that reaction was not complete even when 10-fold excess of PPh_3 in respect to rhodium was used.

To check the stability of heterogenized catalysts, the samples were refluxed in toluene or in toluene containing 20-fold excess of free triphenylphosphine. Such conditions could facilitate eventual removal of rhodium from the carrier to the solution. The above described tests has been conducted for the catalysts on both supports, A and B. From the analytical data (ICP and EDAX) collected in the table 3 one may conclude, that $\text{Rh}(\text{CO})_2^+$ complex is quite stable on both supports (A and B) and only ca. 10% of rhodium was removed from carrier during refluxing in toluene. At the presence of free PPh_3 the samples were found to be less stable and rhodium leaching ca. 16% from A and 35% from B was determined (table 3). Supported cation $\text{Rh}(\text{CO})(\text{PPh}_3)^+$ was less stable and up to ca. 50% of rhodium was leached (table 3). Although both forms of the support (A and B) are structurally quite similar, nevertheless the form A of macroporous lumps, was found better suited for heterogenization of rhodium homogeneous catalysts. Compared with form B the form A has at least two advantages, which are higher rhodium concentration and higher resistance against leaching. Therefore for catalyst testing reactions mainly $\text{Rh}(\text{CO})_2^+/\text{A}$ samples

Table 4
Products of 1-hexene reactions catalyzed by $\text{Rh}(\text{acac})(\text{CO})_2$ supported on A and B under CO/H_2

[1-hexene]:[Rh]	2-Hexene (1%)	Aldehydes (n + iso)(%)
<i>Rh(CO)2+/A</i>		
5710	88	5
4000	88	6
3080	88	4
2030	80	9
1560	89	8
<i>Rh(CO)2+/B</i>		
2200	35	—
1140	74	0.5

Note: Reaction conditions: 80 °C, 10 atm H_2/CO , 6 h.

Table 5

Products of 1-hexene reactions (isomerization and hydroformylation) catalyzed by $\text{Rh}(\text{acac})(\text{CO})_2$ and $\text{Rh}(\text{acac})(\text{CO})(\text{PPh}_3)$ supported on A under CO/H_2 at the presence of PPh_3

$[\text{PPh}_3]:[\text{Rh}]$	Catalyst pre-activation procedure under CO/H_2 or CO atmosphere at the absence of 1-hexene	2-Hexene(%)	Aldehydes ($n + \text{iso}$)(%)	n/iso
<i>Catalyst $\text{Rh}(\text{acac})(\text{CO})_2$ on A</i>				
1.1	No pre-activation	45.5	50.8	2.71
1.2	1.5 h, 10 atm CO/H_2	45.2	50.5	2.73
1.2	3 h, 1 atm CO/H_2	41.8	48.0	2.82
6.3	3 h, 10 atm CO/H_2	30.6	60.6	3.90
1.1	24 h, 1 atm CO	67.6	26.5	2.62
1.1	24 h, 1 atm CO then 24 h, 1 atm N_2	21.8	65.9	2.31
1.2	1 h, 5 atm CO , 80 °C	55.1	34.0	2.78
1.1	2 h, 5 atm CO , 80 °C	82.9	12.6	2.82
1.1	2 h, 5 atm CO , 80 °C	40.2	42.2	2.88
1.0 ^a	No pre-activation	45.0	24.7	1.73
<i>Catalyst: $\text{Rh}(\text{acac})(\text{CO})(\text{PPh}_3)$ on A</i>				
–	No pre-activation	64.5	15.8	2.83
–	3 h, 10 atm CO/H_2 , 80 °C	57.6	15.5	2.78

Note: Reaction conditions: 80 °C, 10 atm H_2/CO , $[\text{1-hexene}]:[\text{Rh}] = 1900$, 4 h.

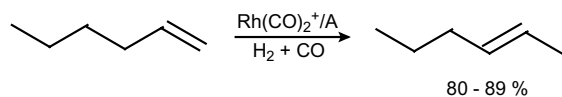
^a Pcy_3 was used instead of PPh_3 .

were used, being first standardized by 2 h refluxing in toluene (table 4).

3.3. Catalytic activity of rhodium complexes supported on alumina–zirconia support in isomerization of 1-hexene to 2-hexene

Isomerization of 1-hexene was observed at hydroformylation reaction conditions (10 atm of $\text{H}_2/\text{CO} = 1$, 80 °C). Results obtained for both catalysts, $\text{Rh}(\text{CO})_2^+/A$ and $\text{Rh}(\text{CO})_2^+/B$, gathered in table 5, show higher conversions (over 90% of 1-hexene) for $\text{Rh}(\text{CO})_2^+/A$.

Changes of $[\text{1-hexene}]:[\text{Rh}]$ concentration ratio from 5700 to 1560 have no effect on reaction yield (80–89% of 2-hexene) and selectivity (only 4–9% of aldehydes).

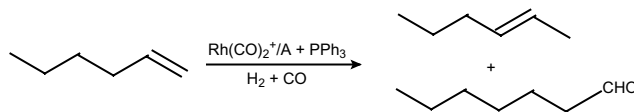


$\text{Rh}(\text{CO})_2^+/B$ catalyst was less active and the yield of 74% of 2-hexene was obtained when relatively high concentration of rhodium ($[\text{1-hexene}]:[\text{Rh}] = 1140$) was applied. It is worth to note that $\text{Rh}(\text{CO})_2^+$ supported on $\text{Al}_2\text{O}_3\text{--ZrO}_2$ presented higher activity than its analog supported on spinel ZnAl_2O_4 , which did not react with 1-hexene at the absence of free PPh_3 . Although 1-hexene isomerization instead of hydroformylation was dominating in the catalytic system under studies the results obtained show undoubtedly reactivity of the catalyst in dihydrogen activation and possible rhodium - hydride intermediate species formation on the surface of $\text{Al}_2\text{O}_3\text{--ZrO}_2$ support.

The carefully filtrated post-reaction solution was used for the next reaction with the new portion of 1-hexene, however only 3% of 2-hexene were found after 6 h at 80 °C and 10 atm H_2/CO . This result confirm the stability of the supported catalyst and the lack of rhodium leaching.

3.4. Catalytic activity of $(\text{Rh}(\text{CO})_2^+/A) + \text{PPh}_3$ in hydroformylation of 1-hexene

Very significant increase of activity (ca. 50% of aldehydes) was observed when to the heterogenized $\text{Rh}(\text{CO})_2^+/A$ catalyst free PPh_3 $[\text{PPh}_3]:[\text{Rh}] = 1.1\text{--}1.2$ was added (table 5).



Even relatively low concentration of PPh_3 added to the system partially retards isomerization (up to 50% of 2-hexene) but significantly increases yield of aldehydes, up to ca. 50%. Pre-activation of catalyst with H_2/CO before introduction of 1-hexene to the autoclave does not influence on the composition of reaction products. However application of higher concentration of PPh_3 , $[\text{PPh}_3]:[\text{Rh}] = 6.3$, cause further increase of the aldehydes yield up to ca. 60% ($n/\text{iso} = 3.9$). Pre-activation of $\text{Rh}(\text{CO})_2^+/A$ in CO atmosphere was found as the way to increase reaction selectivity. For example, pre-activation of $\text{Rh}(\text{CO})_2^+/A$ with CO (24 h, 1 atm CO or 2 h at 5 atm CO in 80 °C) increased the yield of 2-hexene to 67.6% and 82.9%, respectively (table 5), but it decreased the yield of aldehydes. However, when

$\text{Rh}(\text{CO})_2^+/\text{A}$ was pre-activated with CO (1 atm, 24 h), then stored in N_2 atmosphere for 24 h and next used in hydroformylation of 1-hexene – the yield of aldehydes increased to 65.9% ($n/\text{iso} = 2.31$). The obtained results demonstrate uncommon sensitivity of heterogenized rhodium catalyst towards CO. Most reasonable explanation is that CO is blocking rhodium coordination sites making bonding and activation of dihydrogen molecules less effective. The competition of CO and 1-hexene to reach an active sites is less important and therefore isomerization reaction is not inhibited by CO.

Additional coordination of CO to $\text{Rh}(\text{CO})_2^+/\text{A}$ was recorded in IR spectra measurements of the sample of catalyst stored several hours in CO atmosphere. A new intensive $\nu(\text{CO})$ band at 2050 cm^{-1} was observed besides two frequencies at 2011 and 2083 cm^{-1} . The intensity of this band decreases significantly when the sample is left for several hours in N_2 atmosphere. Similar behavior was observed for samples stored during the first few weeks on the air and next, left in CO atmosphere. IR spectra of these samples showed three frequencies at 2011 , 2050 and 2083 cm^{-1} . It is interesting to note that both samples of $\text{Rh}(\text{CO})_2^+/\text{A}$ catalysts (freshly prepared and regenerated in CO atmosphere) presented similar catalytic activity. Application of PCy_3 , to modify $\text{Rh}(\text{CO})_2^+/\text{A}$ catalyst gave worse results when compared with PPh_3 (table 5).

The results of XPS studies of the catalysts led to the conclusion that electronic structure of rhodium in immobilized catalyst $\text{Rh}(\text{CO})_2^+/\text{A}$ is changed under influence of H_2/CO atmosphere. In the spectrum of the sample warmed up in H_2/CO (10 atm) the BE of Rh 3d was shifted towards lower values by -0.45 eV (figure 6, table 2). Smaller shift, by -0.22 eV was obtained for the sample of $\text{Rh}(\text{CO})_2^+/\text{A}$ warmed up in H_2/CO atmosphere at the presence of PPh_3 (figure 6, table 2). The BE shift towards lower values in both samples may suggest some contribution of reduced rhodium.

It is worth to note, that the solution obtained after separation of the supported catalyst was not catalytically active as it was confirmed by the reaction with the new portion of 1-hexene. In this experiment only 2% of 2-hexene were found after 4 h of reaction at 80°C and 10 atm H_2/CO .

3.5. Catalytic activity of $\text{Rh}(\text{CO})(\text{PPh}_3)^+/\text{A}$ in hydroformylation of 1-hexene

In the table 5 are presented some results of 1-hexene hydroformylation with $\text{Rh}(\text{CO})(\text{PPh}_3)^+/\text{A}$ catalyst. At the 1-hexene hydroformylation reaction conditions the isomerization was the main process and ca. 60% of 2-hexene was obtained. Pre-activation of catalyst caused small decrease of yield of 2-hexene but not changed the yield of aldehydes (in both cases ca. 16% of aldehydes were produced).

4. Conclusions

The nanostructured $\text{Al}_2\text{O}_3\text{--ZrO}_2$ mixed oxides, prepared by sol-gel process have been found as good supports for rhodium complexes, $\text{Rh}(\text{acac})(\text{CO})_2$ and $\text{Rh}(\text{acac})(\text{CO})(\text{PPh}_3)$.

Above complexes were supported as cations $\text{Rh}(\text{CO})_2^+$ and $\text{Rh}(\text{CO})(\text{PPh}_3)^+$. The rhodium content, determined by UV-vis, ICP and EDAX methods, was equal ca. 1% and ca. 0.5%, respectively. The stability of supported catalysts during refluxing in toluene or in toluene with excess of PPh_3 is dependent on the method of support preparation (sample A and B). The higher stability was observed for freeze - dried support of macroporous lumps structure (sample A).

The samples of catalysts before use were always standardized by 2 h reflux in toluene. The catalytic tests performed with $\text{Rh}(\text{CO})_2^+$ supported on A at 80°C and 10 atm H_2/CO have shown its high activity in isomerization of 1-hexene to 2-hexene (up to 89%). Modification of the catalyst with PPh_3 ($[\text{PPh}_3]:[\text{Rh}] = 1.2$) led to increase of aldehydes yield up to 65% under the same conditions. The leaching of rhodium was excluded, because the post-reaction solution separated from the catalyst produced only traces (2–3%) of 2-hexene.

It is interesting to note, that the presence of zirconia has positive influence on the reactivity of supported rhodium complex in comparison with earlier studied spinel support, ZnAl_2O_4 [11].

Acknowledgments

This work was supported by Polish State Committee for Scientific Research (KBN) with the PBZ-KBN 15/T09/99/01D.

Authors thank to Mr. Xavier Cessarato from ENSC Clermont – Ferrand, France, for the catalytic reactions performance.

References

- [1] B. Cornils and W.A. Herrmann, in: *Applied Homogeneous Catalysis with Organometallic Compounds*, eds. B. Cornils and W.A. Herrmann (Wiley/VCH, New York, 1996).
- [2] A. Choplin and F. Quignard, *Coord. Chem. Rev.* 178 (1998) 1679.
- [3] J.M. Basset, F. Lefebvre and C. Santini, *Coord. Chem. Rev.* 178 (1998) 1703.
- [4] A.J. Sandee, J.N.H. Reek, P.C.J. Kamer and P.W.N.M. van Leeuwen, *J. Am. Chem. Soc.* 123 (2001) 8468.
- [5] S. Rojas, P. Terreros and J.L.G. Fierro, *J. Mol. Catal. A: Chem.* 184 (2002) 19.
- [6] H. Gao and R.J. Angelici, *J. Mol. Catal. A: Chem.* 145 (1999) 83.
- [7] H. Gao and R.J. Angelici, *Organometallics* 17 (1998) 3063.
- [8] C. Bianchini, D.G. Burnaby, J. Evans, P. Frediani, A. Meli, W. Oberhauser, R. Psaro, L. Sordelli and F. Vizza, *J. Am. Chem. Soc.* 121 (1999) 5961.
- [9] P.W.N.M. van Leeuwen, A.J. Sandee, J.N.H. Reek and P.C.J. Kamer, *J. Mol. Catal. A: Chem.* 182 (2002) 107.

- [10] E. Lindner, F. Auer, A. Baumann, P. Wegner, H.A. Mayer, H. Bertagnolli, U. Reinohl, T.S. Ertel and A. Weber, *J. Mol. Catal. A: Chem.* 157 (2000) 97.
- [11] J. Wrzyszczyk, M. Zawadzki, A.M. Trzeciak and J.J. Ziolkowski, *J. Mol. Catal. A: Chem.* 189 (2002) 203.
- [12] A.M. Trzeciak, J.J. Ziolkowski, Z. Jaworska-Galas, W. Miśta and J. Wrzyszczyk, *J. Mol. Catal.* 88 (1994) 13.
- [13] J.M. Dominguez, J.L. Hernandez and G. Sandoval, *Appl. Catal. A: Gen.* 197 (2000) 119.
- [14] Yu.S. Varshavsky, T.G. Cherkasova and Zh. Neorg. Khim. 12 (1967) 1709.
- [15] F. Bonati and G. Wilkinson, *J. Chem. Soc.* (1964) 3156.